Effect of pH and Dodecylamine Concentration on the Properties of Dodecylamine Two-Phase foam

[1,2]Weimin Xie, [2,3]Dongsheng He*, [3]Shuang Liu, [2]Fei Chen, [2]Hongqiang Li
[1]*Centre for Mineral Materials, School of Minerals Processing and Bioengineering, Central South University, Hunan, Changsha 410083, China*
[2]*School of Xingfa Mining Engineering, Wuhan Institute of Technology, Hubei, Wuhan 430073, China..*
[3]*Key Laboratory of Rare Mineral, Ministry of Land and Resources, Hubei, Wuhan, 430074, China*.
csuhy@126.com*

(Received on 3rd May 2019, accepted in revised form 25th November 2019)

Summary: Over-stabilized foam has always been a problem that plagues the dodecylamine (DDA) flotation system. In this study, a new device, "automatic foam analyzer", was successfully used to characterize the behavior of foam in DDA solution. The effects of pH and DDA dosage on the foam properties were investigated from four aspects: bubble diffusion capacity, Bikerman coefficient, half-life period and solution conductivity, and the mechanism of pH and DDA concentration on foam properties was analyzed by solution chemistry and surface tension of DDA, then the change process of foam structure was deduced. The results showed that the foaming property and stability of DDA bubbles were the best at pH=8. Simultaneously, with the increase of DDA dosage, the foaming property of bubbles was enhanced, the half-life was prolonged, and the foam stability was also improved.

Keywords: Dodecylamine (DDA); Two-phase foam; Foaming property; Foam stability; Characterization device.

Introduction

For both technically and economically, flotation has been regarded as the most effective solution to separate mineral particles on the basis of their wetting properties [1-4]. Moreover, surfactants play an indispensable role in the flotation process and are commonly used as collectors and frothers [5-7]. In this process, the selective adsorption of the collector on the desired mineral surface plays a vital role in the recovery of valuable minerals from the gangue [8, 9].

Since about 40% of common minerals are silicate minerals [10], and some silicate minerals should be inhibited or activated by surfactants to extract useful minerals. Worldwide, the reverse flotation method is considered to be an effective technique for obtaining silicate minerals such as kaolinite, pyrophyllite and illite [11-13], in which cationic surfactants are adsorbed on the surface of silicate minerals by electrostatic adsorption, and they can float out effectively [14,15]. Alkyl amines and their various derivatives are widely used as cationic collectors for the reverse flotation of quartz from different types of minerals such as phosphates and iron oxides [16]. Among these surfactants, Dodecylamine (DDA), a charge-based physisorption collector, has been frequently used for desilication process of reverse flotation [17], such as collecting quartz [18], due to low cost, high efficiency, strong frothing property and high temperature resistance [19-21]. However, using cationic collectors such as DDA also exists some problems, mainly including rich foam, high viscosity and difficult to dissipate [22]. Therefore, the interactions between DDA and bubbles should not be ignored. Corona-Arroyo et al researched the effect of the cationic surfactant dodecyl amine on the bubble size and gas holdup in a two-phase gas-liquid system in a laboratory downflow column [23]. Zhu et al studied bubble aspect ratios and rising velocities of dodecylamine (DDA), methyl isobutyl carbinol (MIBC), sec-octyl alcohol (2-octanol), DDA-MIBC blend, and DDA-2-octanol blend for different concentrations [24]. Zhou et al reported gas holdup and froth height in the presence of dodecylamine at three pH values [25]. Hence, it is of great significance to carry out the study of foam properties of DDA flotation system and to provide a theoretical basis for the rational use of DDA collectors.

Understanding the role and evolution of DDA molecules at air/water interface is the key step to establish a model for industrial flotation processes. Current major efforts on flotation focus on recovery response, and few studies have focused on the law of the bubbles. Therefore, this study aims to provide a better

*To whom all correspondence should be addressed.

understanding of the factors affecting performance of gas-liquid two-phase foam in DDA system. The effects of pH and DDA dosage on bubble property were investigated, and the evolution of the bubble morphology during the flotation process has been discussed.

Experimental

Materials and methods

DDA foam properties test

Instrument

The instrument used in the test was JPM2012 Foam Analyzer (Shanghai Powereach Digital Technology Equipment Co., Ltd.), with the specification of 690 × 310 × 480mm, which consisted of quartz glass tube, optical system, conductance system and air pump. Built-in digital camera that took pictures automatically at regular intervals, and then capturing images. The measuring height was 0-280 mm, and the oil-free air compressor was attached to the equipment, filling air into the device. The test was carried out in a quartz glass tube with a height of 280 mm, an inner diameter of 45 mm and an outer diameter of 55 mm. Along the glass tube, five conductivity measuring probes were used to measure the electrical conductivity at different heights, and the conductivity resolution was 0.01μs/cm. The instrument was connected to the computers to make it easy to observe the shape and height of the foam at any time and to calculate the relevant parameters.

Test method

The test was carried out in the foam analyzer, the principle of which was similar to the air flow method [26].

pH experiments

A series of pH solutions with pH values close to 2, 4, 6, 8, 10, 12 and DDA solutions (chemically pure, Aladdin Chemical Reagent Co., Ltd.,) with a concentration of 3×10^{-2} mol/L were prepared. In a typical experiment process, 24 mL of pH solution was added to the quartz glass tube with a graduated cylinder, and then 1mL DDA solution was dripped with pipetting. Then the glass tube was accessed to the device, click the "Start Test" button, the air is introduced automatically through the air generating device, fix the air flow rate 300mL/min, set the blowing time 50s, and the test temperature is controlled at 25 ℃. When the half-life of the bubble appeared, click "End Test" and saved the image. The computer automatically calculated the parameters of bubble diffusion capacity, foaming performance, Bikerman coefficient and solution conductivity according to the video images. Each solution was measured three times to obtain an averaged value.

DDA dosage experiment

According to the above pH experiment, the appropriate pH value was selected for the DDA dosage experiment, and distilled water was directly used here. The DDA solution having a concentration of 3.0×10^{-2} mol/L was prepared, then gradually diluted to obtain several DDA solutions with the concentration of 3×10^{-4}, 6×10^{-4}, 9×10^{-4}, 12×10^{-4} and 15×10^{4} respectively. Typically, 25 mL DDA solution was added to quartz glass tube with a graduated cylinder, then the glass tube was accessed to the device, click the "Start Test" button, the air is introduced automatically through the air generating device, fix the air flow rate 300mL/min, set the blowing time 50s, and the test temperature is controlled at 25 ℃. When the half-life of the bubble appeared, click "End Test" and saved the image. Each solution was measured three times to obtain an averaged value.

Foam diffusion ability (F_E): refers to the ability of the foam to diffuse outwards by overcoming the forces between foam and foam or between foam and solution.

$$F_E = \frac{V_{Ffoam}}{(V_{iliq} - V_{fliq})} \qquad \text{(Eq. 1)}$$

Bikerman coefficient (IB): The ratio of final foam volume to air flow rate [27]. The larger the foam expansion coefficient, indicating that the higher the foam quality, the stronger the foaming property.

$$IB = \frac{V_{Ffoam}}{D_{Fgas}} \qquad \text{(Eq. 2)}$$

Bubble half-life period: The time requires to reduce the height of the foam by half after it stops inflating, which is used to characterize the stability of the foam, that is, the persistence of the foam after its generation [28].

Conductivity (C_f): Based on the foam is composed by a large number of bubbles separated by a liquid film, in which the liquid phase is conductive and

the gas phase is non-conductive, so that the solution conductivity is taken as a measure of the bubble density, and the information of foaming ability and foam stability of the solution is obtained from the variation law of conductivity [29].

$$C_f = 100 * \frac{C_{tfoam}}{C_{tlip}} \quad \text{(Eq. 3)}$$

V_{Ffoam}—Final foam volume; V_{iliq}—Initial liquid Volume; V_{fliq}—Final liquid volume;

D_{Fgas}—Final air flow; C_{tfoam}—T time foam conductance; C_{tliq}—T time liquid conductance

Surface tension test

The surface tensions of the DDA solution at different concentrations were measured using a JK99c Surface Tension Meter by the plate method. The tension meter was firstly soaked in solutions. In order to avoid the effects of residues, the platinum plate was cleaned successively with alcohol and water, and then flame dried. After that the solution was poured into the measuring container to stabilize for 10 min before the measurement. The room temperature was remained constant throughout the entire measurement. After the balance was reached, the values were recorded. Each solution was measured three times to obtain an averaged value.

Result and Discussion

Effect of pH

The pH of pulp is an important factor affecting the flotation index (calculated according to Eq. 1, 2, 3, the following is the same), the effects of pH on the foam parameters were investigated. The test results are shown in Fig.1, and the dosage of DDA is 1.2×10^{-3}mol / L. The results of Fig. 1a, b and c show that the trend of bubble diffusion capacity, foam Bikerman coefficient and foam half-life, respectively, of which the curves are similar. With the increase of pH, the bubble diffusion capacity, Bikerman coefficient and the half-life gradually increase at first and then decrease piecemeal, and reach the maximum value at about pH = 8. Fig. 1d is the curve of solution conductivity curve, the solution conductivity curve is just opposite to Fig.1 a, b and c. At pH = 2, the conductivity of the solution is the highest, which means that there is less foam and more liquid in DDA system. At pH = 4~10, the solution conductivity is low, indicating that the foam content is very high at this time, while the liquid content is quite small.

Effect of DDA dosage

Then, the effect of the dosage of DDA on the foam parameters was examined (Fig.2). As the amount of DDA increases, the foam diffusion capacity and foam Bikerman coefficient (Fig.2a and b) increase first and then become substantially stable, which is related to the decrease of the surface tension of the solution by adding DDA. But when the DDA dosage reaches a certain concentration, the surface tension of the solution would no longer decreases, and the corresponding foam stability also tends to be constant [30]. From Fig.2c, it can be seen that, with the increases of the dosage of DDA, the half-life of the foam increases gradually, and when the DDA dosage is 12×10^{-4}mol/L, the half-life is the longest, 48s, indicating that the foam is the most stable at this time. It can be seen that the conductivity of the solution (Fig.2d) decreases with the increase of the amount of DDA, and then increases slightly, which shows that the amount of foam production increases first and then decreases with the increase of the dosage of DDA.

Solution chemistry of the DDA

DDA is an organic polar compound containing a negative trivalent nitrogen atom in its molecular structure. It is also called cationic surfactant due to its hydrophobic group after dissociation [25]. DDA has the following equilibrium in solution [31]:

Dissolution equilibrium:

$$C_{12}H_{25}NH_{2(s)} \rightleftharpoons C_{12}H_{25}NH_{2(aq)} \quad \text{(Eq. 4)}$$

$S=[C_{12}H_{25}NH_{2(aq)}]=10^{-4.70}=2\times10^{-5}$mol/L

Acidic electrolysis equilibrium:

$$C_{12}H_{25}NH_3^+ \rightleftharpoons C_{12}H_{25}NH_{2(aq)} + H^+ \quad \text{(Eq. 5)}$$

$$K_a = \frac{[C_{12}H_{25}NH_2]\cdot[H^+]}{[C_{12}H_{25}NH_3^+]} = 10^{-10.63} = 2.3\times10^{-11}$$

Basic electrolysis equilibrium:

$$C_{12}H_{25}NH_2 + H_2O \rightleftharpoons C_{12}H_{25}NH_3^+ + OH^- \quad \text{(Eq. 6)}$$

$$K_b = \frac{[C_{12}H_{25}NH_3^+]\cdot[OH^-]}{[C_{12}H_{25}NH_2]} = 10^{-3.37} = 4.3\times10^{-4}$$

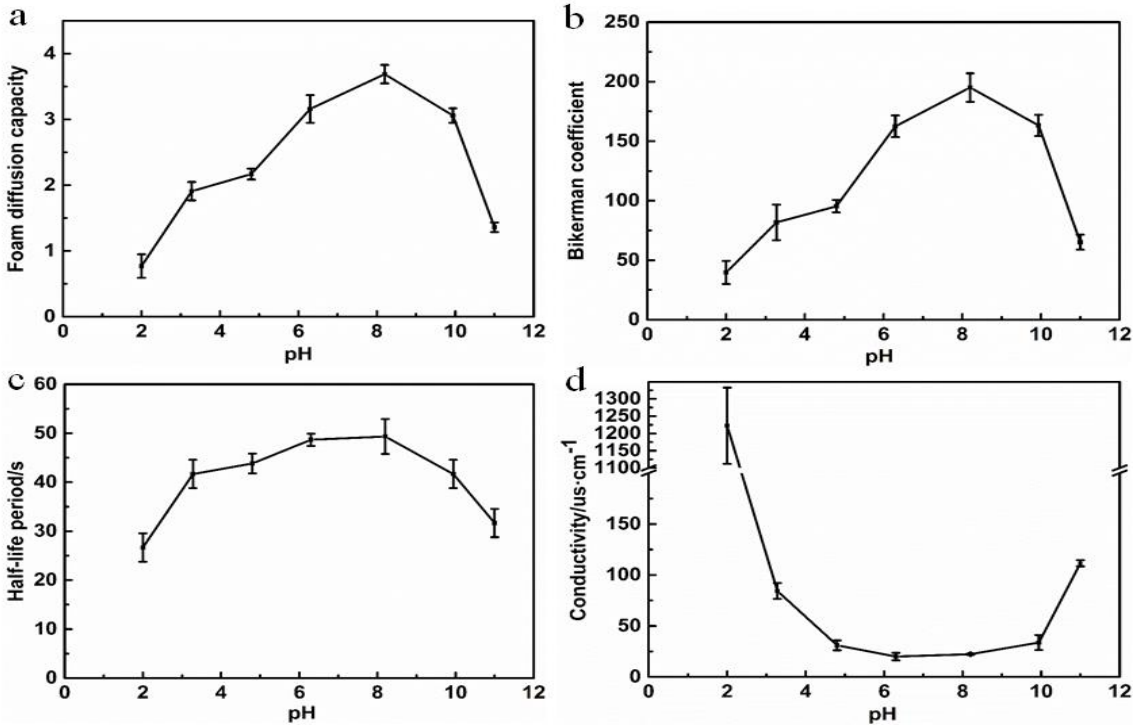

Fig. 1:The relationship between pH and foam diffusion capacity(a); Bikerman coefficient (b); foam half-life period (c); solution conductivity(d) (the DDA dosage is 1.2×10^{-3}mol / L).

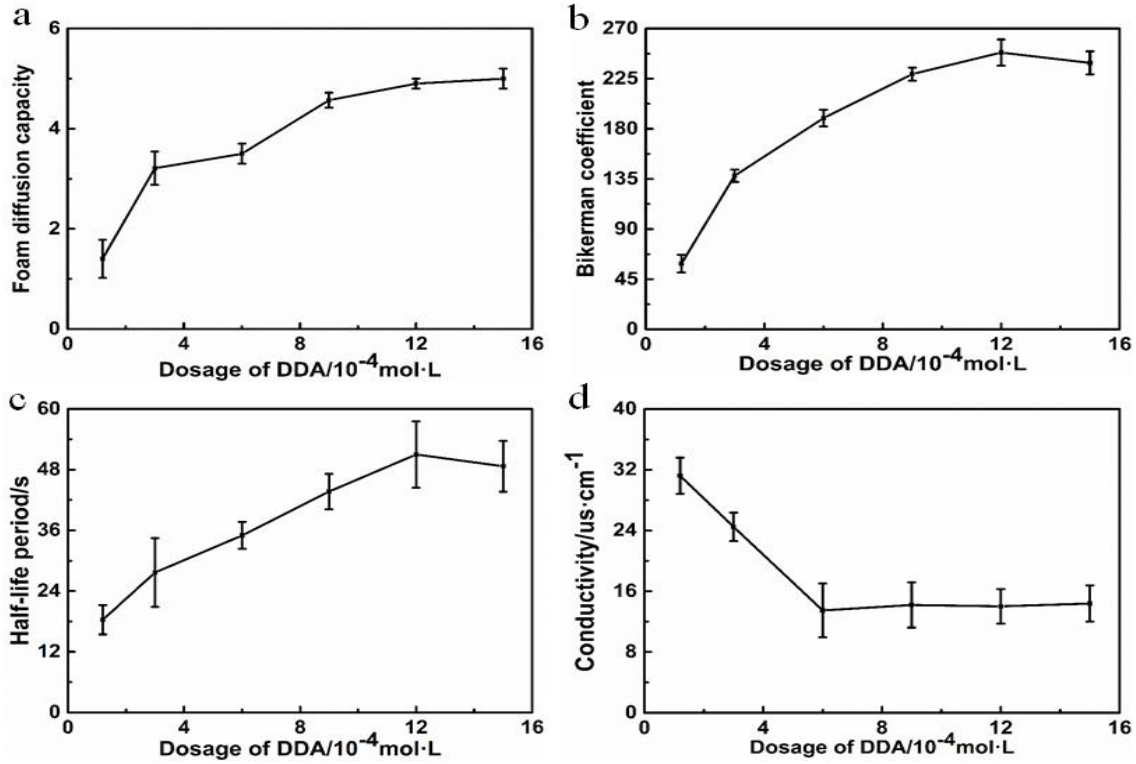

Fig. 2: The relationship between the dosage of DDA and foam diffusion capacity(a); Bikerman coefficient (b); foam half-life period (c); solution conductivity(d) (direct use of distilled water).

The mechanism of the DDA action

Based on the solution equilibrium of DDA (Eq.4, 5, 6), the concentration-logarithmic distribution diagram was drawn (Fig. 3). Obviously, in the floatation of minerals with DDA, both the amine molecules and the amine ions existed simultaneously in the slurry solution, but the concentrations of the two were not the same, and the pH value of the solution varies greatly. In the range of strong alkalinity, the solution was mainly composed of amine molecules, and the solubility of the amine molecules was far less than that of the amine ions, resulting in poor foaming property of the DDA system. In the range of strong acidity, with the addition of H_2SO_4, the concentration of H^+ increased, the repulsive force between hydrophilic groups increased, the surface energy of the system increased and the surface activity decreased, thus weakening the foaming ability of the DDA solution [31]. Therefore, the DDA had better foaming property under weak acid or weak base conditions, which was consistent with the results of Fig. 1.

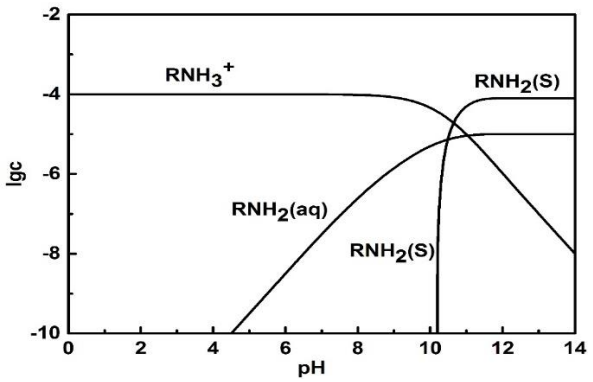

Fig. 3: The logarithmic concentration equilibrium diagram of each component of DDA at different pH values.

The surface tension of the DDA solution

When the foam is formed, the energy (surface energy) of the system increases with the increase of the liquid surface area; when the foam breaks, the energy of the system decreases accordingly. Therefore, from the energy point of view, the low surface tension is advantageous for the formation of the foam, since less work can be performed when a foam having a certain total surface area is generated, but it is not guaranteed that the generated foam has good stability. This can be explained by the Laplace equation (Eq. 7) of the relationship between liquid pressure and curvature: the pressure difference between the Plateau junction of the foam liquid film and the plane film is directly proportional to the surface tension, and the low surface tension leads to small pressure difference and slower drainage rate, and the thinning of the liquid film is also slower, which is conducive to foam stability [32].

$$\Delta P = \gamma\left(\frac{1}{R1} + \frac{1}{R2}\right) \qquad \text{(Eq. 7)}$$

where γ is the surface tension coefficient of the liquid, R is the bubble radius.

The relationship between the surface tension and concentration of the DDA aqueous solution was shown in Fig. 4. The results showed that when a small amount of DDA was added, the surface tension of the aqueous solution dropped sharply. When the concentration of DDA reached 1.0×10^{-3} mol/L, the surface tension of the solution slowly decreased and began to form a platform. At this point, the surface tension of the solution was the minimum tension value of surfactant DDA, which was 9.481N/m. Corresponding to Fig. 2, the foam stability reduced slightly at this time. It could be concluded that the foaming and stability of the foam were the best under the DDA dosage was 1.2×10^{-3} mol/L.

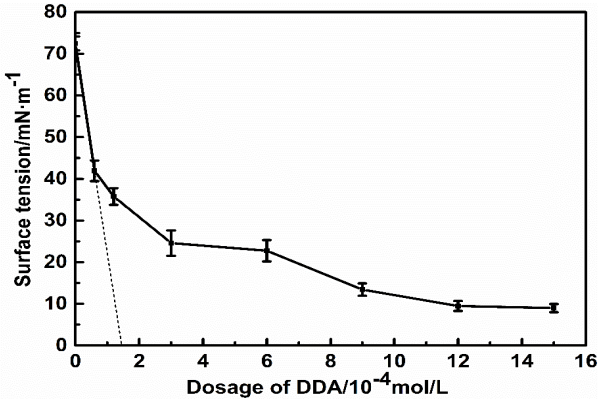

Fig. 4: The relationship between DDA concentration and surface tension (Direct use of distilled water, 25℃)

The analysis of the change process of foam structure

It can be seen from the above test that the foam has better foaming performance and stability at pH=8 and DDA dosage of 1.2×10^{-3}mol / L (lower than the critical micelle concentration of 1.2×10^{-2}mol

/ L [33]). Therefore, the variation of foam height (maximum) is investigated under the optimum conditions (Fig.5), and the black shadow part represents foam height. With continuous inflation, the height of the foam increases gradually. At 50 seconds, the inflation is stopped and the foam height reaches the maximum. Then, the foam height descends gradually. This indicates that the height of the foam is mainly determined by the inflation time. The liquid images of the foam corresponding to each stage in Fig. 5 are shown in Fig. 6, reflecting the generation and disintegration process of bubbles. Within 0 to 50s, the amount of foam is more and more with constant inflation, and the bubbles are dense and small. After stopping charging, the bubbles begin to merge and deform, the volume of the bubbles becomes larger, and the contour between bubbles and bubbles is clearly visible. According to the change of foam height after 50s in Fig. 5, it can be included that the bubbles shattered gradually from inside to outside, from bottom to top.

Fig. 7 is a magnification diagram of the foam change process, from which the shape and change process of the foam can be clearly seen, which including the foaming, growth, drainage, and collapse of foams. Fig. 7a is the process of inflating into the beaker and the foam is gradually generating, which is close to circle at this time; Fig. 7b shows the shape of the foam after inflation, the bubble begins to grow and gradually evolves into a stable state. it can be seen that the walls of the foam begin to move and merge to achieve force balance and the foam has a regular geometry during the floating process, hexahedron; Fig. 7c is the change in the shape of the foam after a period of time, the hexagonal shape of the foam can be clearly seen and enlarged compare Fig.7b, indicating that the bubble begins to merge; Fig. 7d is the regression process of foam, at this time the bubbles merge with each other in a polygonal shape, and infinitely close to a circle.

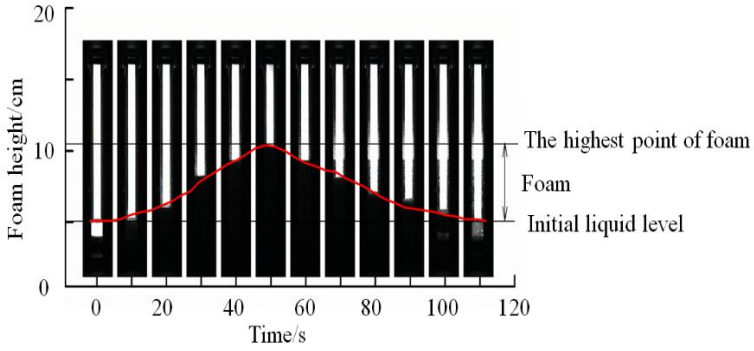

Fig. 5: The relationship between foam height and time (pH=8, DDA dosage is 1.2×10^{-3}mol / L)

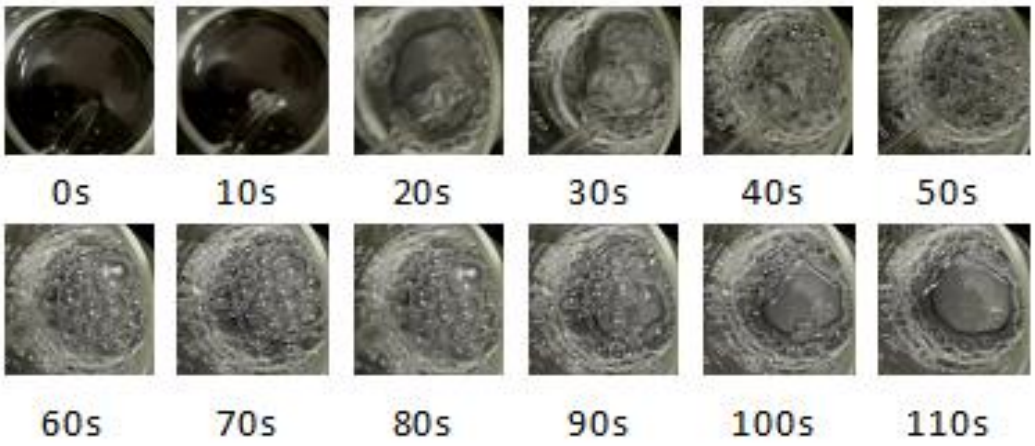

Fig. 6: The generation and destruction process of the bubble (pH=8, DDA dosage is 1.2×10^{-3}mol / L).

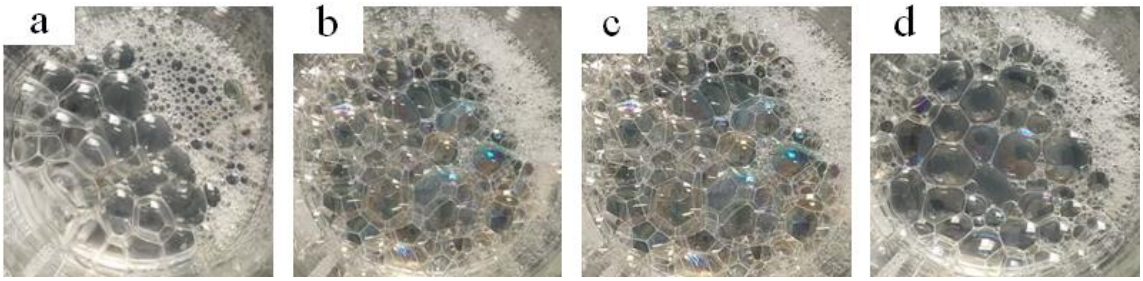

Fig. 7: The change process of foam (pH=8, DDA dosage is 1.2×10^{-3}mol / L).

According to the experimental phenomena in Fig. 5-7, combined with the theory of the formation and collapse of the foam, the evolution process of the foam is inferred, the schematic diagram is shown in Fig. 8. The bubble is divided into the following five stages from the production to gradual disintegration. (a) Aerated in the DDA system, when the air is filled into the DDA aqueous solution, the gas will be cut into several air masses of different sizes and shapes. Due to DDA molecules are amphiphilic, they are easy to enrich in the gas-liquid interface and arrange in a directional arrangement. Then the air masses will be surrounded by the gas-liquid interface arranged with a large number of DDA molecules, and the shape tends to be spherical, forming a stable sub-liquid bubbles [34, 35]. Then the bubbles are gradually going up by buoyancy, liquid film becomes thinner and the volume of the bubble increases. (b) The vast majority of bubbles are floating, On the one hand, they squeeze each other and deform to the most stable hexagonal [36, 37]. This is because the pressure difference is the least when the angle between the liquid films is 120° according to the Plateau boundary, and the foam is most stable, so the foam is mostly hexagonal [38, 39]; On the other hand, the DDA molecules on the surface layer of the bubble in the liquid attract each other and then adhere, and the adhesion of the bubble will squeeze out a thin layer of water, and then the gas in one bubble will diffuse through the hydrated film to another, leading the merger of bubbles. And the small bubbles will gradually become larger through the merger process [40, 41]. (c) Caused by gravity, foam begins to drain, which is the passage of liquid through a foam. During foam drainage, the liquid is confined in a network of channel or plateau borders, which join at a node in four [42]. Therefore, the liquid level rises gradually, the hydration layer among the bubble moves away, and the shape of the bubble changes; (d) With the progress of the liquid film drainage and the influence of gravity, the surface layer gradually consumes, the water-filling amount of the foam surface layer is reduced from the bottom to the top [43], and the bubbles continue to merge, transform from hexagons to polygons; (e) The annexing bubbles reach a short relative equilibrium state, the bubbles are infinitely close to the circle. During this process, the air pressure in the bubble will decrease and the volume of the bubble will increase. When the surface layer is consumed to a thickness of less than 10 nm, it will be easily broken [44].

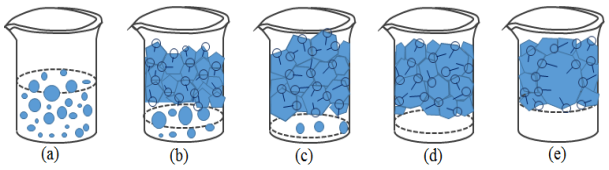

Fig. 8: The schematic diagram of bubble from formation to disintegration.

Conclusions

The foamability and stability of the aqueous solution of DDA increased firstly and then decreased with the increase of pH, and the foaming property and stability were the best at pH = 8. The foaming property of the DDA aqueous solution was related to the concentration of the DDA. When the concentration of DDA was less than 3×10^{-4}mol /L, the foaming property was very poor. When the concentration of DDA was greater than 3×10^{-4}mol/L, the foaming ability increased slowly with the increase of DDA concentration. And the foam stability increased gradually with the increase of DDA concentration. When the concentration of DDA was 1.2×10^{-3}mol/L, the foam stability was the best. Continue to increase the concentration of DDA, the foam stability changed little. In the DDA system, the effect of pH on foamability and stability of foams was greater than that of DDA dosage.

Acknowledgements

This work was financially supported by the Research Fund Program of Key Laboratory of Rare Mineral, Ministry of Natural Resources (No. KLRM-KF202001); Hubei Tailings (Slag) Resource Utilization Engineering Technology Research Center Project (No. 2019ZYYD070)；Hubei Technology Innovation Project (Foreign Science and Technology Cooperation; No. X19S012); China Geological Survey Project (No. DD20190626)

References

1. L. O. Filippov, V. V. Severov and I. V. Filippova, An overview of the beneficiation of iron ores via reverse cationic flotation, *Int. J. Miner. Process*. **127**, 62 (2014).
2. W. G. Liu, W. B. Liu, X. Y. Wang, D. Z. Wei and B. Y. Wang, Utilization of novel surfactant N-dodecyl-isopropanolamine as collector for efficient separation of quartz from hematite., *Sep. Purif. Technol*. **162**, 188 (2016).
3. K. Q. Shu, L. H. Xu, H. Q. Wu, S. Fang, Z. J. Wang, Y. B. Xu and Z. Y. Zhang, Effects of ultrasonic pre-treatment on the flotation of ilmenite and collector adsorption, *Miner. Eng.* **137**, 124 (2019).
4. S. Fang, L. H. Xu, H. Q. Wu, J. Tian, Z. Y. Lu, W. Sun and Y. H. Hu, Adsorption of Pb (II)/benzohydroxamic acid collector complexes for ilmenite flotation, *Miner. Eng.* **126**, 16 (2018).
5. H. Zhang, W. G. Liu, C. Han and D. Z. Wei, Intensify dodecylamine adsorption on magnesite and dolomite surfaces by monohydric alcohols, *Appl. Surf. Sci*. **444**, 729 (2018).
6. V. Ravichandran, C. Eswaraiah, R. Sakthivel, S. K. Biswal and P. Manisankar, Gas dispersion characteristics of flotation reagents, *Powder. Technol*. **235**, 329 (2013).
7. Zhou, A. Jordens, F. Cappuccitti, J. A. Finch and K. F. Waters, Gas dispersion properties of collector/ frother blends, *Miner. Eng*. **96**, 20 (2016).
8. W. Kracht, Y. Orozco and C. Acuna, Effect of surfactant type on the entrainment factor and selectivity of flotation at laboratory scale, *Miner. Eng*. **92**, 216 (2016).
9. W. G. Liu, W. B Liu, S. J. Dai and B. Y. Wang, Adsorption of bis(2-hydroxy-3-chloropropyl) dodecylamine on quartz surface and its implication on flotation, *Results. Phys.* **9**, 1096 (2018).
10. G. H. Li, H. G. Dong, C. M. Xiao, X. H. Fan, Y. F. Guo and T. Jiang, Mineralogy and separation of aluminum and iron from high ferrous bauxite, *J. Cent. South. Univ*. **02**, 235 (2006).
11. H. Jiang, Z. Sun, L. Xu, Y. Hu, K. Huang and S. Zhu, A comparison study of the flotation and adsorption behaviors of diaspora and kaolinite with quaternary ammonium collectors, *Miner. Eng*. **65**, 124 (2014).
12. S. Fang, L. H. Xu, H. Q. Wu, Y. B. Xu, Z. J. Wang, K. Q. Shu and Y. H. Hu, Influence of surface dissolution on sodium oleate adsorption on ilmenite and its gangue minerals by ultrasonic treatment, *Appl. Surf. Sci*. **500**, 144038 (2020).
13. L. Xu, Y. Hu, F. Dong, Z. Gao, H. Wu, Z. Wang, Anisotropic adsorption of oleate on diaspore and kaolinite crystals: implications for their flotation separation, *Appl. Surf. Sci*. **321**, 331 (2014).
14. L. Xu, Y. Hu, J. Tian, H. Wu, Y. Yang, Z. Wang and J. Wang, Selective flotation separation of spodumene from feldspar using new mixed anionic/cationic collectors, *Miner. Eng.* **89**, 84 (2016).
15. H. Jiang, Y. Gao, Q. H. Yang, S. A. Khoso, G. R. Liu, L. H. Xu and Y. H. Hu, Adsorption behaviors and mechanisms of dodecyltrimethyl ammonium chloride and cetyltrimethyl ammonium chloride on illite flotation, *Powder technology*, **331**, 218 (2018).
16. W. Y. Liu, M. Pawlik, M. Holuszko, The role of colloidal precipitates in the interfacial behavior of alkyl amines at gas–liquid and gas–liquid–solid interfaces, *Miner. Eng.* **72**, 47 (2015).
17. Z. Y. Gao, W. Sun and Y. H. Hu, New insights into the dodecylamine adsorption on scheelite and calcite: An adsorption model, *Miner. Eng.* **79**, 54 (2015).
18. L. Wang, W. Sun, R. Q. Liu, Mechanism of separating muscovite and quartz by flotation, *J. Cent. South. Univ*. **21**, 3596 (2014).
19. A. P. L, Nunes, A. E. C. Peres, A. P. Chaues and W. R. Ferreira, Effect of alkyl chain length of amines on fluorapatite and aluminium phosphates floatabilities, *J. Mater. Res. Technol*. **8**, 3623 (2019).
20. L. Wang, R. Q. Liu, Y. H. Hu and W. Sun, pH effects on adsorption behavior and self-aggregation of dodecylamine at muscovite/aqueous interfaces, *J. Mol. Graph. Model*. **67**, 62 (2016).
21. Y. Gao, Y. X. Han and W. B. Li, Flotation behavior of diatomite and albite using

dodecylamine as a collector, *Minerals*, **8**, 371 (2018).
22. Y. F. Zhao, Q. T. Lai, Y. F. Liao, Y. C. He, Z. C. Liu, Y. W. Liao and S. H. Ding, Effect of slime on foam stability in ammonium sulfide flotation system, *Conservation and utilization of mineral resources*, **03**, 52 (2017).
23. M. A. Corona-arroyo, A. Lopez-valdivieso, J. S. Laskowski and A. Encinas-oropesa, Effect of frothers and dodecylamine on bubble size and gas holdup in a downflow column, *Miner. Eng.* **81**, 109 (2015).
24. H. Z. Zhu, A. L. Valdivieso, J. B. Zhu, F. F. Min, S. X. Song, D. Q. Huang and S.M. Shao, Effect of dodecylamine-frother blend on bubble rising characteristics, *Powder technology*, **338**. 586 (2018).
25. X. Zhou, Y. H. Tan and J. A. Finch, Effect of pH and time on hydrodynamic properties of dodecylamine, *Physicochem. Probl. Mi*. **54**, 1237 (2018).
26. Y. L. Gu, Study on frother performance and its effect on sulfide flotation, Central South University, p. 20 (2013).
27. N. Barbian, Y. Chen and C. G. Li, Foam stabilized column linking foam stability to flotation index, *Metallic ore dressing abroad*, **08**, 38 (2005).
28. M. M Wang and D. H. Gun, Foamability of foaming agent and effecting factors, *Advances in fine petrochemicals*, **12**, 40 (2007).
29. L. J. Wang, G. Y. Zhang, J. F. Dong, X. H. Zhou and X. L. Hong, Progress in test and evaluation methods for foaming performance, *China surfactant detergent & cosmetics*, **03**, 171 (2005).
30. H. Zhang, C. Han, W. G. Liu, D. X. Hou and D. Z. Wei, The chain length and isomeric effects of monohydric alcohols on theflotation of magnesite and dolomite by sodium oleate, J. Mol. Liq. **276**, 471 (2019).
31. C. Y. Sun and W. Z. Yin, Principle of silicate mineral flotation, Beijing, p. 127 (2001).
32. X. Mu, Study on stability and antifoaming of three-phase foam, Central South University, p. 5 (2005).
33. M. B. M Monte and J. F. Oliveira, Flotation of sylvite with dodecylamine and the effect of added long chain alcohols, *Miner. Eng.* **17**, 425 (2004).
34. J. B. Yianatos and F. Henriquez, Boundary conditions for gas rate and bubble size at the pulp-froth interface in flotation equipment, *Miner. Eng*. **20**, 625 (2007).
35. S. F. Li, M. P. Schwarz, Y. Q. Feng, P. Witt and C. Sun, A CFD study of particle–bubble collision efficiency in froth flotation, *Miner. Eng.* **142**, 105855 (2019).
36. I. Mackay, A. R. Videla and P. R. Brito-Parada, The link between particle size and froth stability - Implications for reprocessing of flotation tailings, *J. Clean. Prod.* **242**, 118436 (2020).
37. A. L. Fameau and A. Saint-Jalmes, Non-aqueous foams: Current understanding on the formation and stability mechanisms, *Adv. Colloid. Interfac.* **247**, 454 (2017).
38. L. P. Wan, Y. F. Meng and X. D Zhao, Mechanism study on stability of foam fluid, *Xinjiang Oil & Gas*., **01**, 70 (2003).
39. C. Li, K. Runge, F. N. Shi and S. Farrokhpay, Effect of flotation froth properties on froth rheology, *Powder. Technol.* **294**, 55 (2016).
40. N. Barbian, K. Hadler, E. Ventura-Medina and J. J. Cilliers, The froth stability column: linking froth stability and flotation performance, *Miner. Eng.* **18**, 317 (2005).
41. B. Huang, G. W. Liu, P. Feng, H. X. Xu and L. X. Zhao, Influence of cations on foaming characteristics and interfacial properties of sodium dodecyl sulfate, *Journal of mining science and technology.* **3**, 76 (2018).
42. J. L. Wang, A. V. Nguyen and S, Farrokhpay, A critical review of the growth, drainage and collapse of foams, *Adv. Colloid. Interfac.* **228**, 55 (2016).
43. S. Ata, N. Ahmed and G.J. Jameson, A study of bubble coalescence in flotation froths, *Int. J. Miner. Process.* **72**, 255 (2003).
44. S. Z. Liu, W. F. Guo and S. Huang, The mechanics analysis about formation, stability and burst of flotation froth, *Journal of Fuzhou University*, **44**, 296 (2016)